INTERACTION NOTES

NOTE 627

October 2015

STUDY OF THE PROPAGATION OF IEMI SIGNALS ALONG POWER AND COMMUNICATION LINES

Nicolas MORA, Gaspard LUGRIN, Farhad RACHIDI

EMC Laboratory

Swiss Federal Institute of Technology in Lausanne (EPFL)

Lausanne, Switzerland

Markus NYFFELER, Pierre BERTHOLET

HPE Laboratory

Federal Department of Defence – Armasuisse

Spiez, Switzerland

Marcos RUBINSTEIN

University of Applied Sciences of Western Switzerland (HEIG-VD)

Yverdon, Switzerland

Corresponding author: nicolas.mora@epfl.ch

Abstract: This note studies the propagation of IEMI (Intentional Electromagnetic Interference) signals along power/communication cables. Specifically, the attenuation and distortion of the IEMI signals resulting from conductive and dielectric losses are studied. The presented analysis allows the evaluation of the required propagation distance at which the attenuation and distortion of IEMI signals are such that traditional SPDs can be effectively used to protect sensitive devices connected at the end of the lines.

TABLE OF CONTENTS

1 INTRODUCTION

This work deals with the evaluation of voltages and currents at equipment terminals that are sensitive to an IEMI attack [1]. IEMI stresses on a system can be applied either through conducted coupling or radiated electromagnetic coupling [2]. In both cases, interferences (either induced or directly injected) will reach the sensitive devices through connected cables.

The propagation of IEMI signals along power and communication lines will be affected by (i) conductive losses and dielectric losses, and (ii) radiation losses. The distorted transmission will result in the modification of the amplitudes and the rise time of the original induced waveform.

In the first part of this study, we assess the attenuation and distortion of selected cables through a simplified Transmission Line (TL) [3] analysis considering uniform lines with conductive and dielectric losses. The radiation losses and reflection due to non-uniformities will not be considered in this work.

For lines using good conductors such as copper or aluminium (as in communication and power cables), the attenuation should be governed by the conductance of the line, which is directly related to the dielectric losses. However, for lines with very small cross-section, the skin effect plays an important role in the attenuation of the signals.

Since it is expected that the disturbances will slow down as they propagate along the lossy lines, in the second part of this work we assess the increase of the rise time and attenuation as a function of the propagation distance so that classical SPDs could be used to mitigate IEMI disturbances.

This work is organized as follows. Section 2 presents the simplified TL model and the selected cross sections for the study. The performed parametric attenuation and dispersion studies are presented in Section 3. The method for estimating the SPD installation distance is presented in Section 4. Finally, the conclusions are presented in Section 5.

2 MODELING CONSIDERATIONS

Consider the differential mode coupling of an electromagnetic disturbance onto a lossy uniform transmission line of finite length *L*. The electromagnetic disturbance is represented as an equivalent lumped source at a given position along the line. In order to simplify the analysis, we will assume that the line is matched at both ends and an equivalent voltage source is used to excite the line at one end, as schematically shown in Figure 1.

The transmission line is characterized by its characteristic impedance Z_0 and its complex propagation constant γ. The propagation transfer function *H* relating the voltages at both ends of the line can be expressed as:

$$H = \frac{V(L)}{V(0)} = e^{-\gamma L} = e^{-\alpha L} e^{-j\beta L}, \qquad (1)$$

where the complex propagation constant γ has been decomposed into the attenuation constant α and the phase constant β.

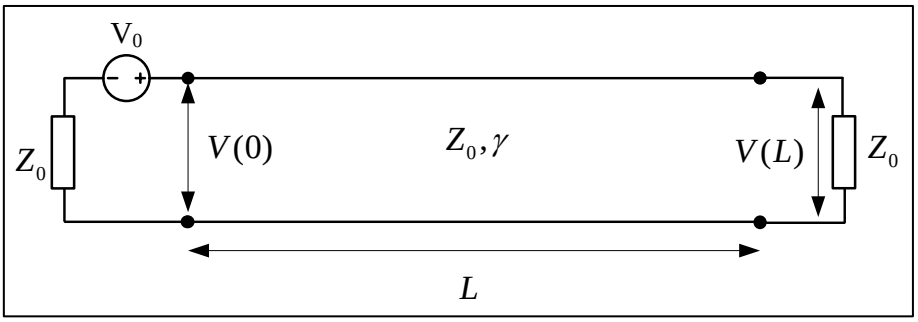

Figure 1 Schematic diagram of a uniform two-wire transmission line excited by an equivalent voltage source representing the differential mode field-to-wire coupling from an external source.

The complex propagation constant of a transmission line can be calculated from its per-unit-length (p.u.l) parameters as [1]:

$$\gamma = j\omega\sqrt{LC}\sqrt{(1-\frac{R'G'}{\omega^2 LC}) - j(\frac{R'}{\omega L'} + \frac{G'}{\omega C'})} \qquad (2)$$

in which R', L', G' and C' are respectively the line p.u.l. resistance, inductance, conductance and capacitance.

2.1 Differential mode propagation cross sections

We studied the transfer function and the complex propagation constant of typical power and communication lines found in civilian installations, namely, (i) low-voltage power lines (LVP), (ii) twisted pairs (TWP), and (iii) radio frequency coaxial lines (RFC).

The cross section definition of the RFC line is shown in Figure 2. In this figure, σ is the conductivity of the inner and outer conductors, ε_r and $\tan\delta$ are the relative permittivity and tangent loss of the dielectric insulator, T is the outer conductor thickness, and r_w and r_s are respectively the radii of the inner conductor and the dielectric insulator.

The cross sections of the LVP and TWP lines are presented in Figure 3. Two wires of radii r_w and conductivity σ are coated with a dielectric insulator with a relative permittivity ε_r and a tangent loss $\tan\delta$. The outer radius of the coating is r_m.

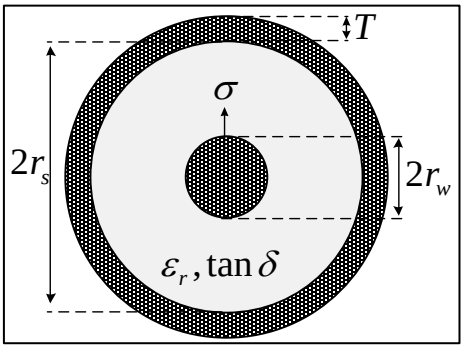

Figure 2 Schematic diagram of the geometry and constitutive materials of a lossy RF coaxial line

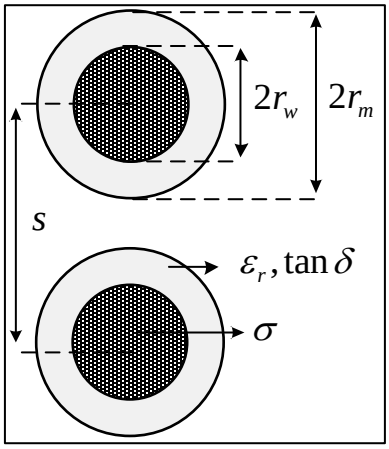

Figure 3 Schematic diagram of the geometry and the constitutive materials of a lossy two-coated-wire line

The p.u.l. parameters of the lines were calculated with classical analytical formulas or fast numerical procedures [1] and were used to run the parametric analyses.

2.2 Effective complex permittivity

The constitutive parameters of the dielectrics were approximated with constant relative permittivity and tangent loss. Neglecting the conduction currents inside the dielectric, the tangent loss can be expressed as:

$$\tan\delta = \frac{\sigma_d + \omega\varepsilon''}{\omega\varepsilon'} \approx \frac{\varepsilon''}{\varepsilon'}, \qquad (3)$$

where ε' and ε'' account respectively for the polarizability of the medium, and the loss (heat) due to the damping of the vibrating dipole moments [2].

Finally, the complex permittivity of the dielectric materials was calculated using:

$$\hat{\varepsilon} = \varepsilon_0(\varepsilon' - j\varepsilon'') = \varepsilon_0\varepsilon_r(1 - j\tan\delta) \qquad (4)$$

2.3 Parameters of selected lines

We have gathered the dimensions and the constitutive materials of several LVP, TWP, and RFC lines for calculating their p.u.l. parameters. The conductors of the considered lines were made of copper with a conductivity $\sigma = 58$ MS/m. The dielectric insulators of the lines varied between polyethylene (PE), polytetrafluoroethylene (PTFE) (Teflon), or polyvinyl chloride (PVC). The relative permittivity and tangent loss of the dielectric insulators at a frequency of 100MHz are given in Table 1.

Table 1 Dielectric properties of constitutive materials

Dielectric	ε_r	$\tan\delta$
PVC	2.3	0.02
PE	2.1	0.8×10^{-3}
PTFE	3	0.4×10^{-3}

A summary of the parameters of each line is presented in Table 2. The first column of the table contains the usual denomination of the lines. The second and third columns present the line type and the used dielectric insulator. The approximated dimensions are contained in the third to sixth column. The approximated characteristic impedance Z_0 of the lines is given in the seventh column. The p.u.l. resistance R' and conductance G' (calculated at a frequency of 1GHz) are shown, respectively, in the eighth and ninth columns. Finally the calculated attenuation factor (in dB/100m) of the lines is shown in the last column.

In order to estimate the attenuation factor, the attenuation constant of the lines was approximated using [2]:

$$\alpha \cong \frac{1}{2}\left(\frac{R'}{Z_0} + G'Z_0\right) \qquad (5)$$

Table 2 Parameters of selected lines

Name	Type	Diel.	r_w [mm]	r_m / r_s [mm]	s [mm]	Z_0 [Ω]	R' [Ω/m]	G' [mS/m]	Att. [dB/100m]
2X1.mm^2	LVP	PVC	0.7	1.200	2.4	90	3.6	2.56	117
2/0 AWG	LVP	PVC	6.3	8.300	16.6	70	0.42	1.94	62
Cat. 5e	TWP	PE	0.29	0.470	0.99	92	9.1	0.11	47
Cat.6	TWP	PE	0.26	0.550	1.12	105	10.1	0.15	49
Cat.7	TWP	PE	0.29	0.700	1.40	103	9.1	0.23	49
RG58	RFC	PE	0.47	1.475	N/A	50	3.7	0.56	44
RG174	RFC	PE	0.24	0.740	N/A	50	7.2	0.57	75
RG316	RFC	PTFE	0.27	0.775	N/A	50	6.6	0.28	63
RG214	RFC	PE	1.13	3.620	N/A	50	1.5	0.55	25

Notice that the LVP lines do not necessarily have a fixed separation distance unless they are grouped inside an insulating jacket. For evaluating the values of the parameters presented in Table 2, the separation distance was approximated to twice the radius of the dielectric. This is used only as an indication of the expected propagation characteristics.

According to Table 2, the conductive and dielectric losses of the studied lines have a considerable magnitude at 1GHz and should be included in the calculation of the propagation of a disturbance at these frequencies. The LVP lines exhibit the highest dielectric losses due to the PVC insulation. On the other hand, TWP have the highest conductive losses due to the small cross section of the lines.

3 PARAMETRIC ANALYSES AND RESULTS

3.1 Numerical simulations setup

In this paper, the transfer functions *H* of three selected lines have been calculated:

(i) 2 x1.5mm2 (LVP),

(ii) Cat 5 (TWP), and

(iii) RG58 cable (RFC)

In order to compare the contribution of the conducive and dielectric losses, the transfer functions were calculated by using the parametric configurations presented in Table 3.

Table 3 Parametric loss configurations

Loss configuration	σ	$\tan\delta$
None	∞	0
Only conductive	$\sigma_{Cu} = 58$MS/m	0
Only dielectric	∞	$\tan\delta_{dK}$
both	$\sigma_{Cu} = 58$MS/m	$\tan\delta_{dK}$

A hyperband signal was used as a voltage source to excite the lines at one end (see Figure 1) and the transmitted voltage at the other end was calculated by convoluting the waveform with the inverse Fourier transform of the transfer function. In what follows, the transmitted voltage and the amplitude of the transfer function are presented for each of the studied lines. The total length of the lines was set to L=10 m. No approximations were made in the calculation of the complex propagation constant. Figure 4 shows the injected signal, which is representative of a hyperband IEMI waveform with a risetime of 229 ps.

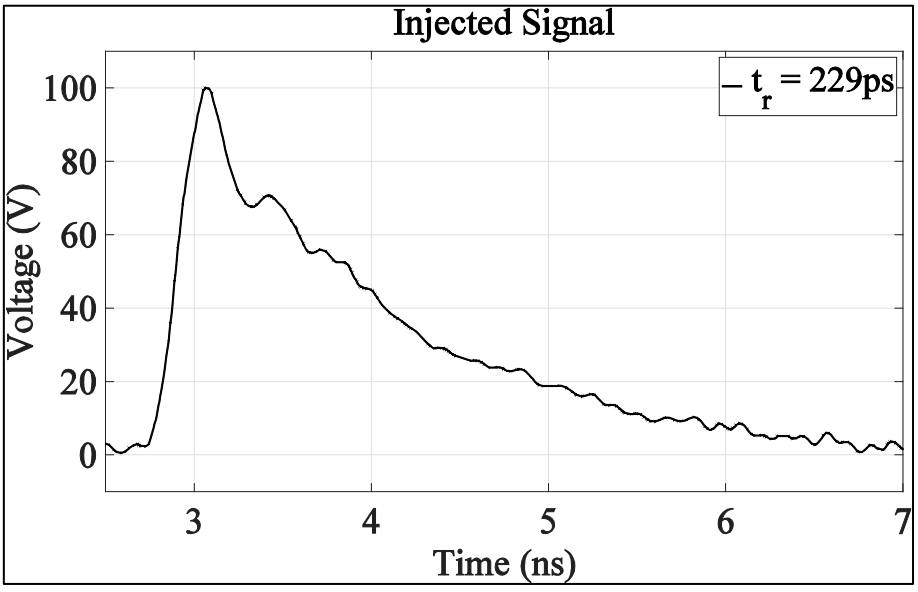

Figure 4 Injected voltage representative of a hyperband IEMI (adapted from [3]).

3.2 Results

The results for the 10-m LVP line are presented in Figure 5. The upper and lower panels present, respectively, the propagated signals at the far end of the line, and the magnitude of the transfer function. The black-dashed curve corresponds to the calculated signal when no losses are included. If the conductive losses are included (blue curve), there is an attenuation of about 10% for the peak amplitude, and an increase in the signal risetime. The attenuation in this case is less than 3dB at the highest frequency.

On the other hand, if only the dielectric losses are considered (green curve), the peak attenuation is about 40% and a more significant increase is observed for the risetime. The attenuation is more than 30 dB in the GHz range. Finally, the red curve shows the results obtained when both losses are included. In this case, the overall peak attenuation is about 50% and the obtained risetime and attenuation are comparable to the values obtained if only dielectric losses are included.

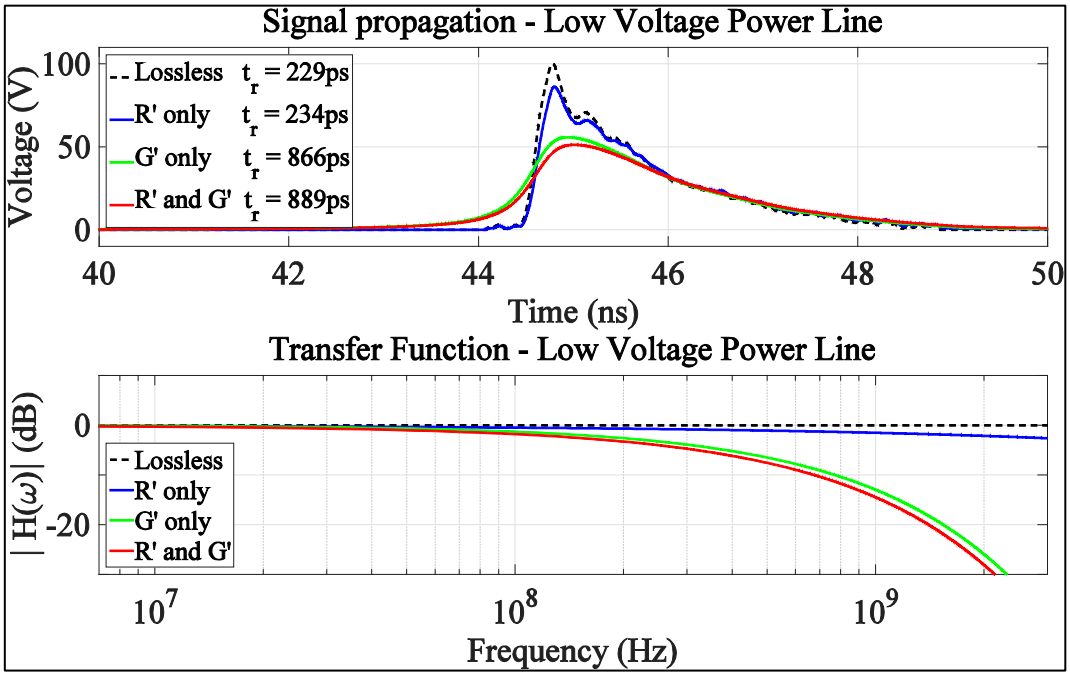

Figure 5 Propagation along a 10-m long LVP line. (a) Transmitted signal (b) Transfer function

The simulation results for the 10-m TWP line are shown in Figure 6. Unlike the case of the LVP line, for which the dielectric losses were predominant, in this case, the conductive losses prevail. This is essentially due to (i) smaller cross section of the wires and (ii) thinner dielectric coating with lower tangent loss for the twisted wires in the network cable in comparison with the power cable. Notice that there is a marginal increase of the risetime, and the attenuation in the GHz range is less than 10 dB.

Finally, the results for the 10-m RFC line are shown in Figure 7. The performance of this line is similar to the TWP case, with predominant conductive losses due to the small cross section

of the inner wire. The effect of the homogeneous padding with dielectric insulator inside the coaxial line can be observed in that the signal arrives 7 to 9 ns later than in the previous cases. Also notice that the dielectric losses are slightly more significant in the GHz range than in the TWP line.

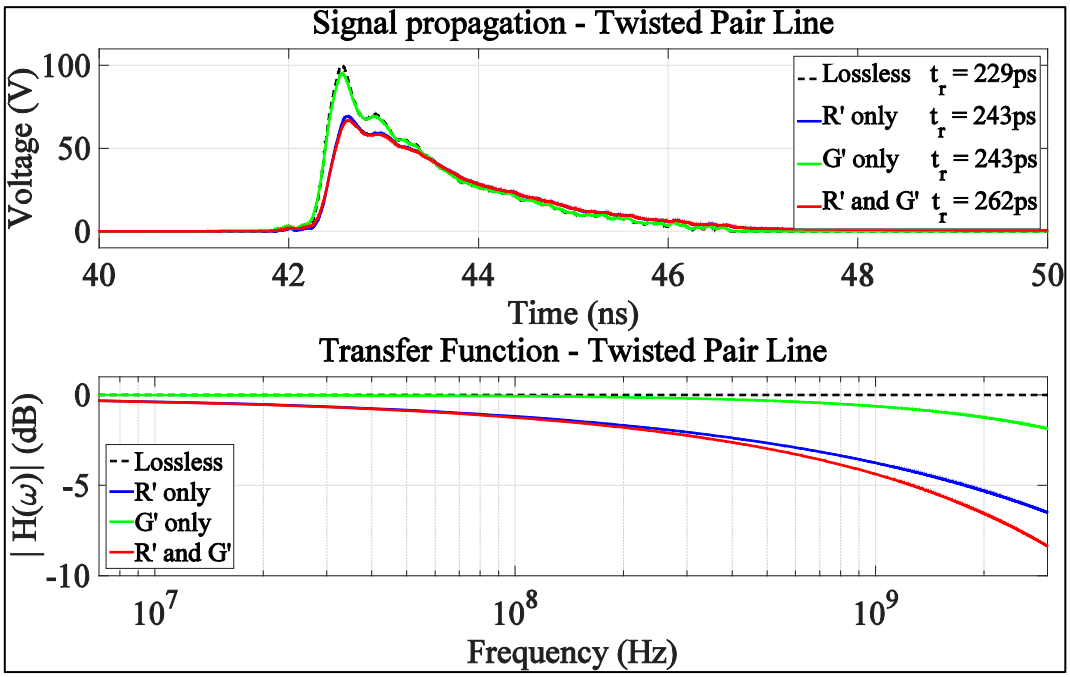

Figure 6 Propagation along a 10-m long TWP line. (a) Transmitted signal (b) Transfer function

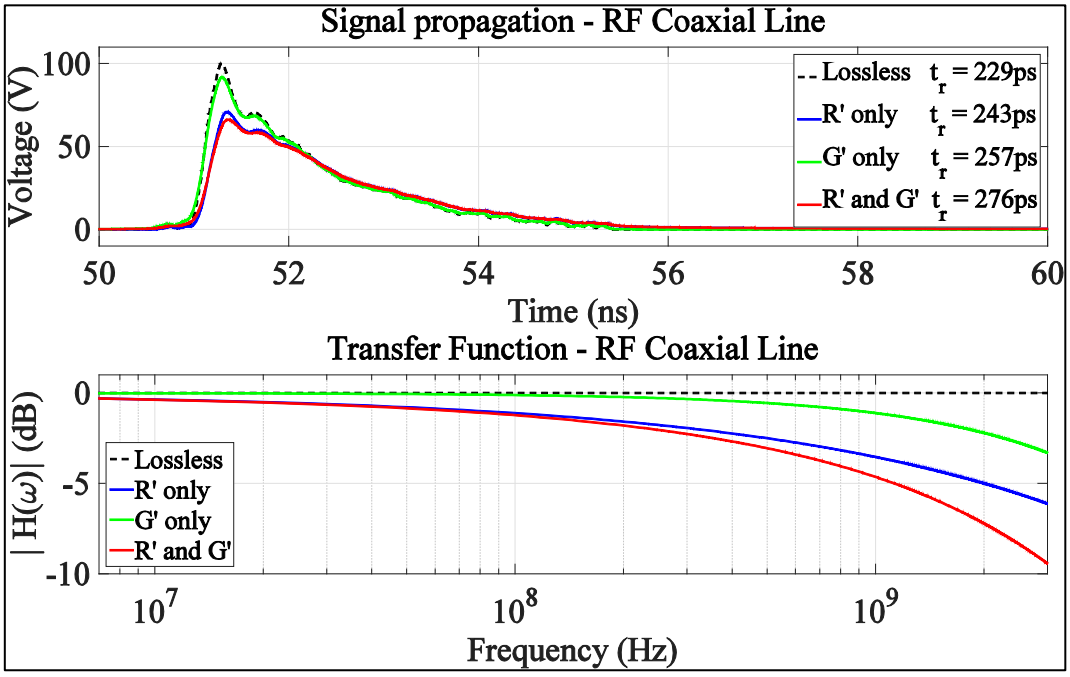

Figure 7 Propagation along a 10-m long RFC line. (a) Transmitted signal (b) Transfer function

4 ON THE POSSIBLE USE OF EXISTING SURGE PROTECTION DEVICES TO MITIGATE IEMI PULSES

According to the results of Section 3, the differential mode propagation of fast transients can be significantly attenuated by the presence of losses in the transmission lines. One of the effects of thick dielectrics coatings is the increase of the risetime with respect to the original waveform.

Traditional surge protection devices (SPDs) are used to protect from disturbances originated by signals that could be slower than the expected IEMI signals (e.g., those originated from ESD, NEMP, or lightning). Therefore, it is useful to assess the propagation distance at which lossy transmission lines will disperse an IEMI-originated disturbance so that classical SPDs could be used. It is also useful to evaluate the required propagation distance to reduce the disturbance amplitude so that less strong SPDs could be installed.

In what follows, we present a method for evaluating the required propagation distance in order to meet the specifications of a given SPD.

4.1 Proposed method

Consider the voltage excitation of the matched transmission line presented in Figure 1. The voltage at the line input is $V(0,\omega) = \mathrm{V}_{in}(\omega)$. Assuming that the installed SPD supports a disturbance $V_{\mathrm{ref}}(\omega)$, the required transfer function of the line is given by:

$$H_{\mathrm{req}} = \frac{V_{\mathrm{ref}}(\omega)}{V_{\mathrm{in}}(\omega)} = e^{-\gamma L_{req}} \tag{6}$$

Neglecting the dispersion caused by the phase delay of the line, the required length for meeting the required transfer function can be derived as follows:

$$\begin{aligned} \left|H_{\mathrm{ref}}\right| &= \left|e^{-\gamma L_{req}}\right| = e^{-\alpha L_{req}} \\ L_{req}(\omega) &= \frac{1}{\alpha(\omega)} \ln\left(\left|\frac{V_{\mathrm{in}}(\omega)}{V_{\mathrm{ref}}(\omega)}\right|\right), \end{aligned} \tag{7}$$

where the fact that the attenuation constant is also a function of frequency has been made explicit.

The length derived in (7) provides the minimum required length so that a specific frequency of the input voltage spectrum is sufficiently attenuated. Notice that since the phase delay of the lines is not considered, no predictions can be made about the expected increase of the risetime.

4.2 Application examples

In order to illustrate the method, we have chosen the same lines that were used for the parametric analysis presented in Section 3. We assumed an injected hyperband disturbance with the characteristics presented in Table 4, and an SPD that supports a disturbance with the characteristics presented in

Table 5. Figure 8 plots a comparison of both waveforms (upper panel) and the spectra (lower panel). Notice that the input disturbance is faster than the SPD specifications. The disturbance has to be attenuated by at least half of the peak amplitude in order to meet the requirements. Also notice that the low frequency spectrum of the input disturbance is already lower than that required by the SPD.

Table 4 Characteristics of the injected disturbance

Parameter	Value
Peak Amplitude	200V
Risetime	400 ps
Duration (FWHM)	2 ns

Table 5 Characteristics of the supported disturbance

Parameter	Value
Peak Amplitude	100V
Rise time	2.4ns
Duration	40 ns

The minimum required lengths for each of the studied lines obtained with (7) are plotted in Figure 9. They exhibit a significant variation as a function of frequency. The required lengths are negative for frequencies below 20 MHz, meaning that below this frequency, the spectrum of the SPD specification is already above the input disturbance spectrum.

In the intermediate frequency range, the required lengths increase rapidly up to about 50 to 70 meters. This means that the intermediate frequency range of the disturbance has to be significantly attenuated in order to meet the requirements. Finally, at higher frequencies, the required lengths decrease to about 10 to 30% percent of the maximum. These are the required lengths to attenuate the early time part of the disturbance.

In order to illustrate the dispersion effectiveness, we have chosen three different lengths for each line type as follows:

(1) The maximum length predicted by Equation (7) (Figure 9).

(2) The length corresponding to the highest significant frequency of the injected disturbance, namely $1/\pi t_r \approx 800\text{MHz}$.

(3) The length that provided attenuation to about half of the disturbance amplitude, determined iteratively.

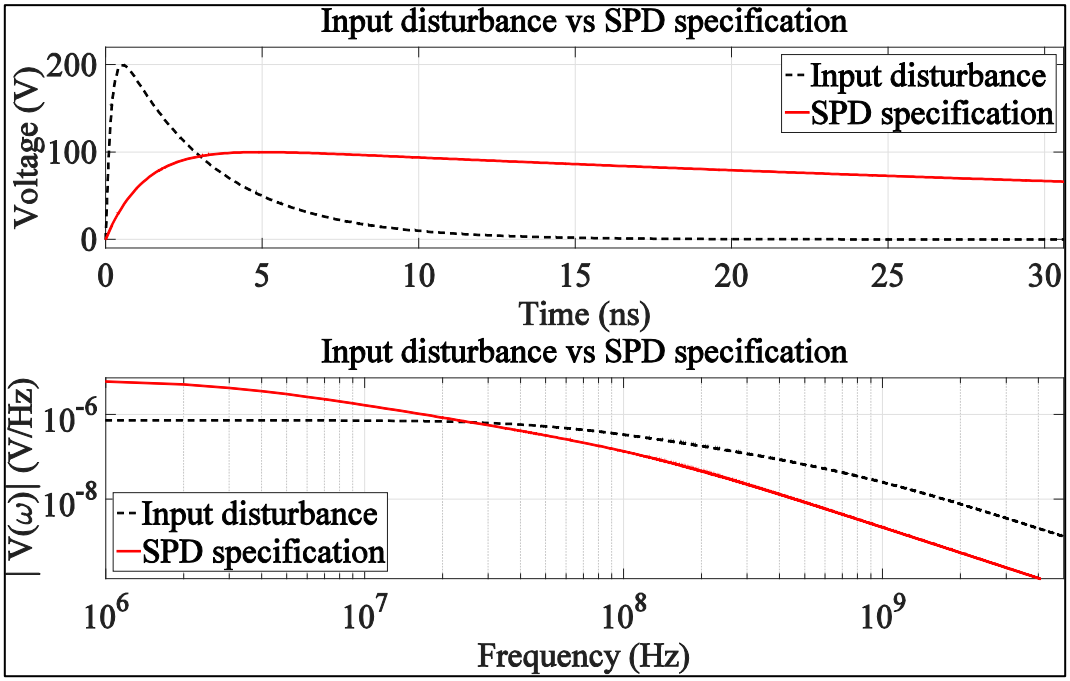

Figure 8 Injected disturbance vs. SPD specifications

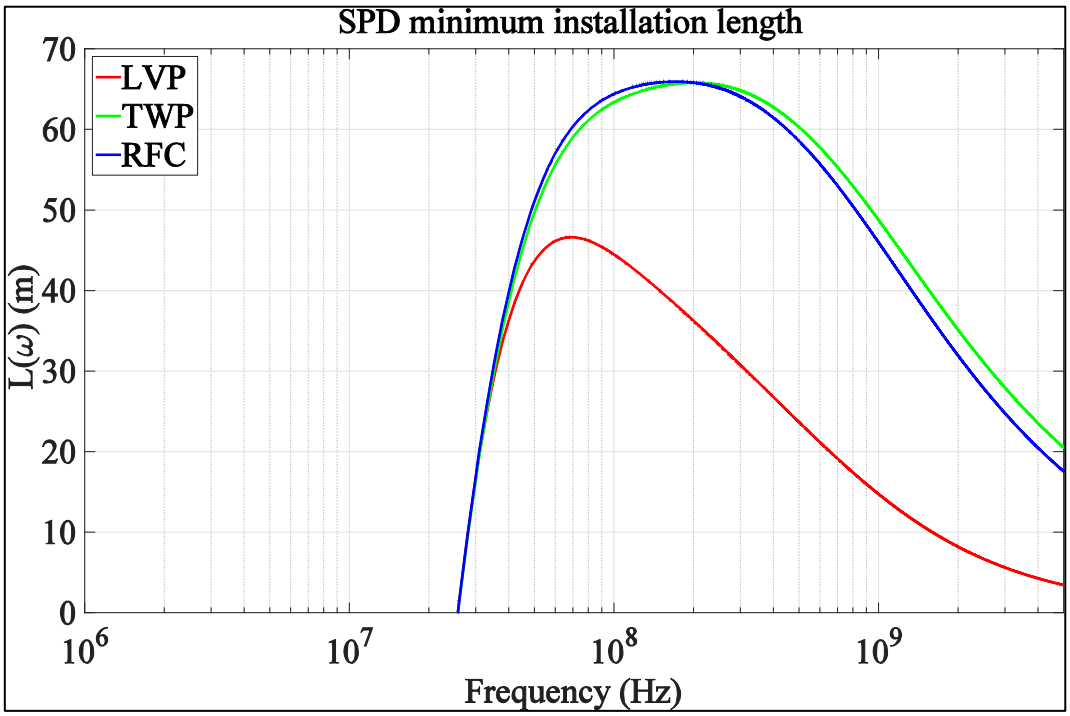

Figure 9 Minimum required length for SPD installation

Figure 10 plots the injected and transmitted disturbances for lines with lengths specified in the legends. The results obtained by considering the LVP line, the TWP line, and the RFC line

are shown in the upper, middle, and bottom panels, respectively. The risetimes of the propagated signals are also indicated in the figures' legend.

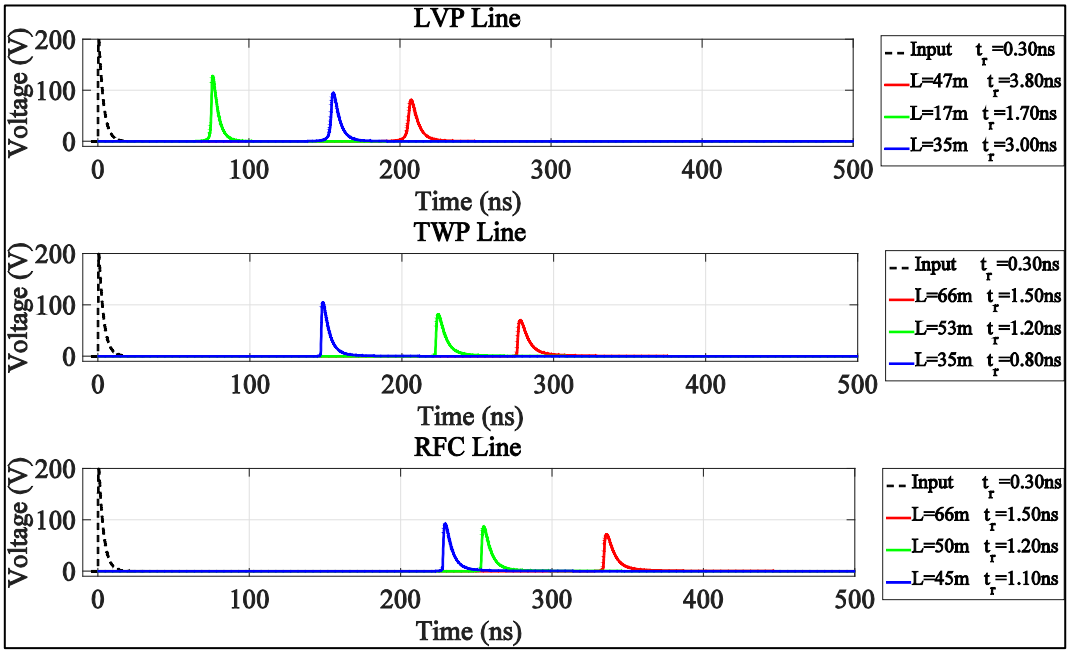

Figure 10 Injected and propagated disturbances in LVP (upper panel), TWP (middle panel), RFC (bottom panel) lines. Red: Results corresponding to the maximum length; Green: Results for the length corresponding to the highest significant frequency of the injected disturbance; Blue: Results corresponding to the length that provided attenuation to about half of the disturbance amplitude, determined iteratively.

In general, the results illustrate that line lengths between 35 to 45 m (blue curves) will attenuate the signal to half of its original amplitude and therefore satisfy the amplitude requirements of the SPD. If the maximum length predicted by Equation (7) is used (red curves), the disturbance will be further attenuated and will also satisfy the SPD amplitude requirements. On the other hand, the risetime requirement is only achieved by the LVP line. The dielectric loss of the TWP and RFC lines is not high enough to slow down the input disturbance to the required limit, for the considered lengths.

5 CONCLUSIONS

The differential mode propagation of very fast injected transients can be significantly affected by the presence of losses in power and communication lines, resulting in an attenuation of the peak and an increase of the risetime. Similar results were obtained in [3-6] where the propagation of IEMI signals in low voltage power networks was assessed from an experimental point of view.

In this work, we studied the effects of including conductive and dielectric losses in the analysis of the differential mode propagation in selected transmission lines. The parameters of several power and communication lines were extracted in order to assess the significance of the conductive and dielectric losses at the expected frequencies of IEMI perturbations. The results show that both dielectric and conductive losses have to be taken into account in order to obtain the total attenuation. However, it has been evidenced that in lines with very small conductor cross-section, it is more likely that the conductive losses will dominate the total attenuation due to the skin effect.

The presented analysis allows the evaluation of the required propagation distance at which the attenuation and distortion of IEMI signals are such that traditional SPDs can be effectively used to protect sensitive devices connected at the end of the lines. An approximate method for identifying the required distance for the installation of a traditional SPD designed for mitigating slower disturbances has also been proposed. The application of the method has been shown through three application examples.

6 ACKNOWLEDGEMENTS

This study was financed by the Armasuisse Science and Technology (Contract Nr. 8003504623).

7 REFERENCES

[1] C. R. Paul, *Analysis of multiconductor transmission lines*. Hoboken, N.J.: Wiley-Interscience : IEEE Press, 2008.

[2] D. M. Pozar, *Microwave Engineering*. Hoboken, NJ: Wiley, 2012.

[3] D. Mansson, T. Nilsson, R. Thottappillil, and M. Backstrom, "Propagation of UWB Transients in Low-Voltage Installation Power Cables," *Electromagnetic Compatibility, IEEE Transactions on*, vol. 49, pp. 585-592, 2007.

[4] D. Mansson, R. Thottappillil, and M. Backstrom, "Propagation of UWB Transients in Low-Voltage Power Installation Networks," *Electromagnetic Compatibility, IEEE Transactions on*, vol. 50, pp. 619-629, 2008.

[5] N. Mora, C. Kasmi, F. Rachidi, M. Darces, and M. Helier, "Modeling of the propagation along low voltage power networks for IEMI studies," in *Electromagnetics in Advanced Applications (ICEAA), 2013 International Conference on*, 2013, pp. 436-439.

[6] N. Mora, C. Kasmi, F. Rachidi, M. Darces, M. Hélier, and M. Rubinstein, "Analysis of the Propagation of High Frequency Disturbances along Low-Voltage Test Raceway," presented at the American Electromagnetics International Symposium (AMEREM), Albuquerque, New Mexico, USA, 2014.